

Original Article

Dual Frequency Tuning of a Microstrip Patch Antenna by Introducing Inclined Slit and Adding an Extra Portion to the Patch

Tilak Sarmah¹, Pranjal Borah², Tulshi Bezboruah³

^{1,3}Department of ECT, Gauhati University, India,

²Department of Instrumentation and USIC, Gauhati University, India,

¹Corresponding Author : zbt@gauhati.ac.in

Received: 21 November 2022

Revised: 02 January 2023

Accepted: 10 January 2023

Published: 29 January 2023

Abstract - The generation of dual-band and the tuning of microstrip antenna is an important aspect of practical applications. In this paper, a technique for the development of an antenna which can be tuned for two bands is described. We propose two techniques, namely: (i) by cutting an inclined slit on the rectangular patch and (ii) by adding an extra portion to the patch. A simple rectangular patch antenna is first designed for its operation in the S-band at 2.4GHz. This is followed by the introduction of an inclined slit of width 100µm on the radiating patch connecting the two edges to transform the original antenna into a dual-band antenna. Next, by adding an extra portion at the upper end of the patch and by varying the dimension of the extra portion, we convert it for dual frequency tuning. Prominent results are observed and are discussed in this paper.

Keywords - Dual band, FR-4 substrate, Inclined, Slit, Tuning.

1. Introduction

Microstrip antenna (MSA) is becoming popular in microwave communication because it meets the emerging challenges with respect to size, performance, and cost. It offers the advantages of lightweight, low profile, ease of fabrication at low cost and compatibility with the integrated circuit. Despite these advantages, one of the foremost drawbacks of the patch antenna is its narrow bandwidth. For advanced communication systems, to meet the diversified requirement for communication, it is necessary to assemble multiple antennas in a device, increasing the system's size and cost. Sometimes, the electromagnetic (EM) incompatibility among different antennae may lead to deterioration of the system stability. To overcome these drawbacks, the multi-band, as well as the reconfigurable antenna, becomes highly desirable. To cover several frequency bands with a single antenna having enough efficiency and bandwidth is a challenge. The only possible solution is the development of a reconfigurable antenna, which tunes for different frequencies. This paper proposes techniques to convert a single-frequency rectangular MSA (RMSA) to a dual-band one by introducing an inclined slit. Then, by adding an extra portion at the upper end of the patch, we make the antenna tunable for dual-frequency operation. Multiple resonances within the same physical geometry are mainly achieved by changing the electrical length for the current distribution on the radiating patch. In their previous work, the authors have shown a simulated work for achieving dual band operation by cutting a slit at an inclination of 45° over the radiating patch presented elsewhere [1].

In the proposed work, we use two techniques, namely: (i) to convert a single antenna to dual resonant frequencies by using a 100µm inclined slit, and (ii) to make the antenna tunable by adding an extra portion to the upper end of the patch. Finally, combining both techniques, we design a dual resonant frequency tunable antenna.

2. Related Works

Various techniques have been developed and reported for achieving dual band operation with a single patch antenna, e.g. by using the shorting post as in [2, 3], stub of different lengths as in [4], meander line technique as in [5], F, E, Y, U, and H shaped antennas as in [6-11,27,37], slit having defected ground structure (DGS) as in [12, 13], the combination of slit and slots as in [14, 15, 16], and multiple arms radiating elements as in [18, 39].

Some researchers used to design reconfigurable antennae by loading multiple split ring resonators as in [19], tuning stub over the patch feed line as in [20, 21], by using radio frequency (RF) MEMS technology as in [22, 40], by using PIN diode and varactor diode as in [24, 25]. Tunable aperture-coupled MSA has been designed and integrated into [26]. A digitally tunable capacitor (DTC) is used to reconfigure an antenna [41]. Insertion of slits on the patch to reconfigure an antenna was reported in [28]. Tuning of the fork-shaped antenna with the n-shaped parasitic element and the partial slotted ground has been presented in [29]. By varying the reverse bias voltage of a varactor diode, the electrical length of the radiating patch can be varied and make the antenna tunable, as reported in



[23,30]. An inverted F-antenna (IFA) having an open slit etched on the top of a plate has been designed and reported in [38,42]. Metamaterial-based monopole patch antenna to tune frequency over a wide bandwidth was proposed in [32]. To reconfigure a dielectric patch antenna, a novel varactor loading scheme has been proposed [17, 33]. Shorting posts are used between the patch and ground plane at different locations to tune an antenna over the entire 5GHz wireless local area network (WLAN) band, as in [34].

3. Materials and Methods

The RMSA is designed to operate in the dominant mode (TM₁₀), which resonates at a frequency of 2.4GHz. Theoretically, the resonant frequency can be calculated from equation (1) as in [43]:

$$f_r = \frac{1}{2\sqrt{\mu_o \epsilon_o}} \sqrt{\left(\frac{m}{a}\right)^2 + \left(\frac{n}{b}\right)^2} \quad (1)$$

Where μ_o = permeability of the medium, ϵ_o = permittivity of the medium, a is the length of the patch, b is the width of the patch, and $m, n = 0,1,2,3\dots$

For dual frequency resonant patch antenna, cutting slit or inserting slots provides two current paths, which leads to two resonant frequencies [36]. Now, the approximated values of the two resonant frequencies in accordance with the two current paths can be calculated from equation (2) and equation (3):

$$f_1 = \frac{v_0}{2L_1\sqrt{\epsilon_r}} \quad (2)$$

$$f_2 = \frac{v_0}{2L_2\sqrt{\epsilon_r}} \quad (3)$$

Where L_1 and L_2 are the average lengths of the current paths of first and second resonant frequencies f_1 and f_2 . v_0 is the speed of light in free space.

The antenna is designed on flame retardant-4 (FR-4) epoxy, and a microstrip line feeding technique is used to excite the patch. After that, a slit with an inclination is introduced on the radiating patch at different positions (p) and with different inclined angles (θ). Fig.1(a) through Fig.1 (d) shows the schematic diagram of the antenna configurations. The design parameters of the proposed antenna are given in Table 1. The " p " is varied in steps of 1mm along the width of the patch from one of the non-radiating edges, as shown in Fig.1 (b).

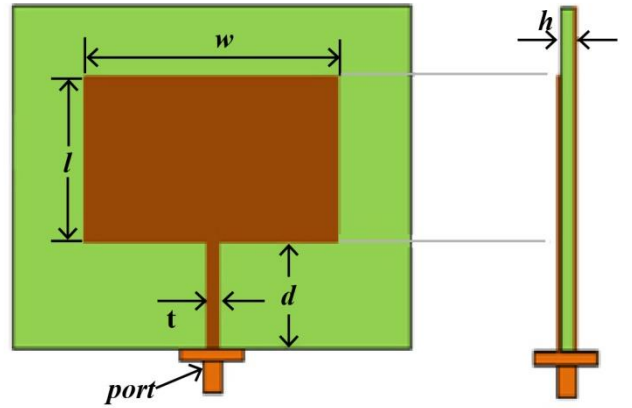


Fig. 1(a) Schematic diagram of a simple RMSA

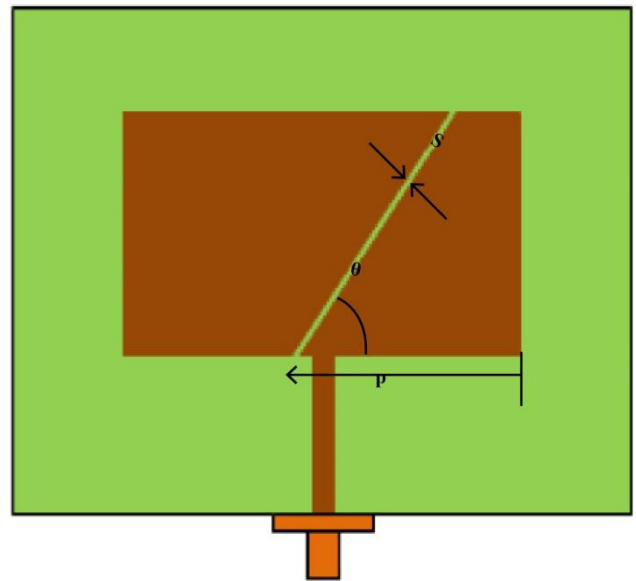


Fig. 1(b) Schematic diagram of a RMSA with the inclined slit.

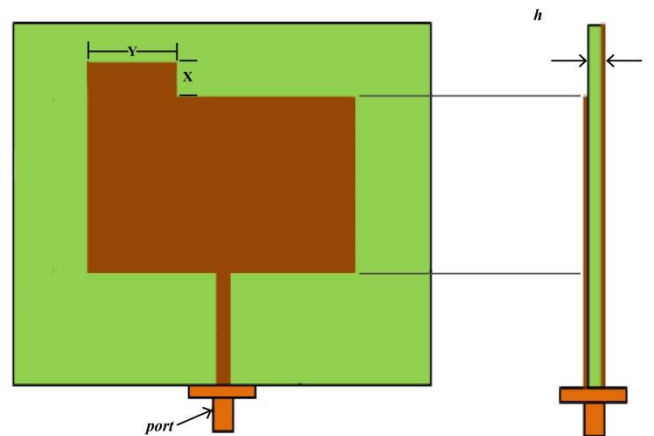


Fig. 1(c) Schematic diagram of a RMSA with an extended portion at the upper end of the patch.

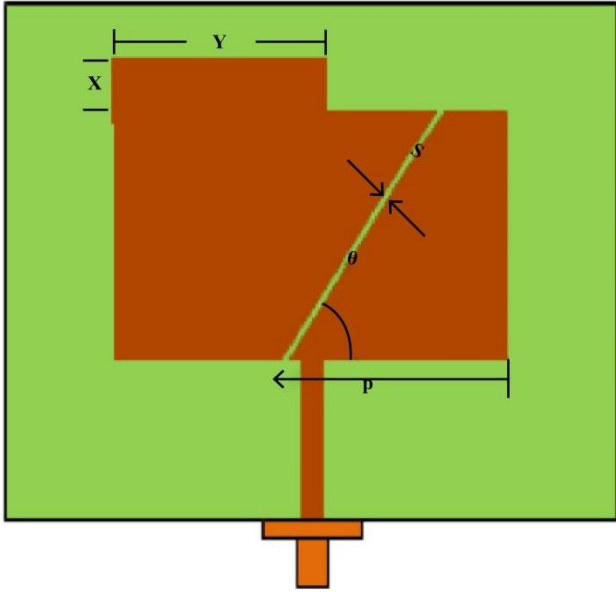


Fig. 1(d) Schematic diagram of a RMSA with the combination of extended portion and inclined slit.

Furthermore, for each value of "p", the angle "θ" is varied within the range of 35° to 85° in steps of 5°, assuring the slit is being inclined over the patch. In the proposed work, out of all the results, we consider the best result where the position of the slit is at a distance of p = 37mm from its edge, having an inclination angle of 70°. With the introduction of the slit, the antenna resonates at dual frequencies of 1.95GHz and 2.44GHz. If we add an extra portion at the upper side of the antenna and vary its dimensions (X and Y), as shown in Fig.1 (c), it becomes tunable. Finally, we design an antenna, as shown in Fig.1 (d), which is a combination of Fig.1 (b) and Fig.1 (c). In the proposed work, we have examined the different parameters of the antenna for the different values of "X" and "Y".

The design parameters of the antenna are given in Table 1.

Table 1. Design parameters of the antenna

Parameters	Values
f_r	2.4 GHz
l	28.2 mm
w	47 mm
h	1.5 mm
s	100μm
t	1.8mm
d	15mm
p	1, ...,47mm
θ	35°, ...,85°
X	3, 6, 9, 12 & 15mm
Y	5, 15, 25,35 & 45mm

The following algorithm is followed to design the proposed antenna:

- Step 1: The frequency range for which the antenna is to be designed is selected.
- Step 2: Pick up the suitable material to design the antenna based on profile, size etc.

- Step 3: Calculate the dimension of the patch for the required specifications.
- Step 4: Design the antenna using any EM simulation software tool and analyze the design.
- Step 5: Optimize it for the best-performed dual frequency antenna by varying the desired parameters ("p" and "θ").
- Step 6: Design the dual resonant frequency antenna by using HFSS.
- Step 7: Introduce an extra portion at the upper end of the patch to tune the antenna.
- Step 8: Optimize for the best-tuned result by varying the dimension of the added portion
- Step 9: STEP 9: Design the antenna and measure the results.

The flow chart for the proposed design is given in Fig. 2

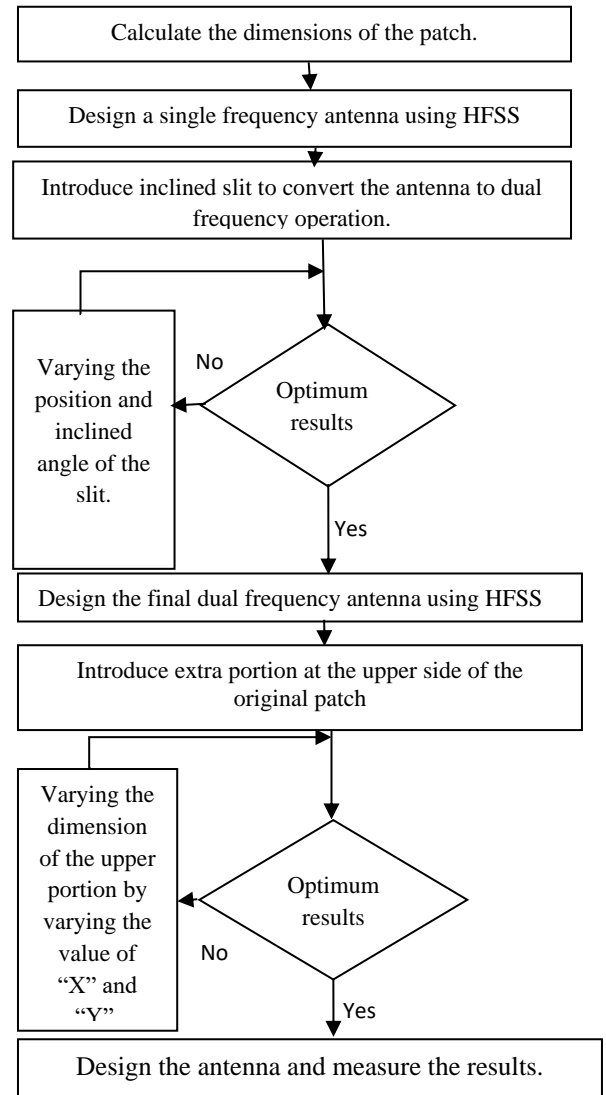


Fig. 2 Flow chart of the proposed design

4. Results and Discussion

A simple patch antenna having 100μm slit at 37mm and 70° inclination is designed, and then by adding an extra portion at the upper end of the antenna, we have simulated different antennas by using HFSS (Version: 13.0). In this work, we analyze the parameters for X =

3mm & 15mm and Y=5mm, 15mm, 25mm, 35mm & 45mm.

4.1 Return Loss Measurement

The simulated return loss for the designed antenna ($p=37\text{mm}$ and $\theta=70^\circ$) with different "X" and "Y" are given in Table 2. It is observed that as the dimension of the upper end is increased, the resonant frequency is shifted towards the lower frequency side. Fig. 3 (a) shows the plot of return loss (S_{11}) in dB versus frequency in GHz for the dimension of the added portion $X = 3\text{mm}$, $Y=5\text{mm}$, 15mm , 25mm , 35mm , and 45mm . Fig.3 (b) shows the same plot for $X=15\text{mm}$, $Y=5\text{mm}$, 15mm , 25mm , 35mm , and 45mm .

It is observed that increasing the dimension of the patch by extending the values of "X" and "Y" increases the antenna's electrical length. As a result, the resonant frequencies are drifted towards the lower frequency end.

Table 2. Observed resonant frequencies and return Loss.

X (mm)	Y (mm)	f_1 (GHz)	$S_{11}(f_1)$ (dB)	f_2 (GHz)	$S_{11}(f_2)$ (dB)
0	0	1.95	-14.10	2.44	-12.20
3	5	2.00	-16.80	2.56	-17.73
	15	2.00	-21.73	2.54	-15.31
	25	2.00	-15.95	2.47	-20.24
	35	1.98	-12.04	2.36	-16.86
	45	1.97	-19.80	2.34	-18.13
15	5	2.00	-18.95	2.52	-18.64
	15	1.99	-18.00	2.50	-18.88
	25	1.83	-2.25	2.11	-9.03
	35	1.60	-14.00	1.88	-13.80
	45	1.60	-25.47	1.72	-19.14

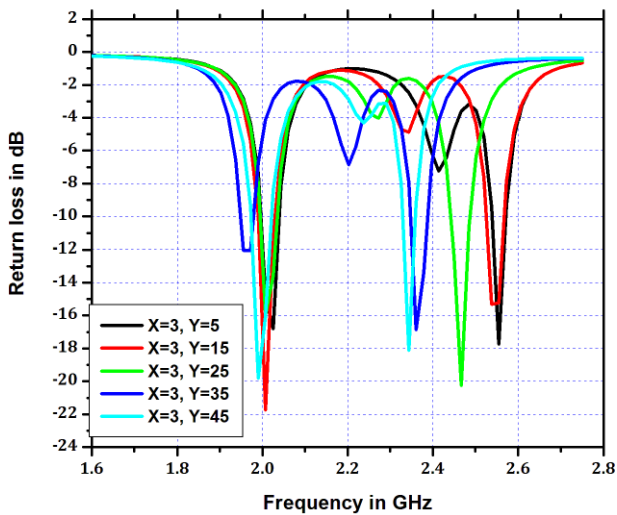


Fig. 3(a) Return loss plots of the patch antenna for X=3mm, Y=5, 15, 25, 35 and 45mm.

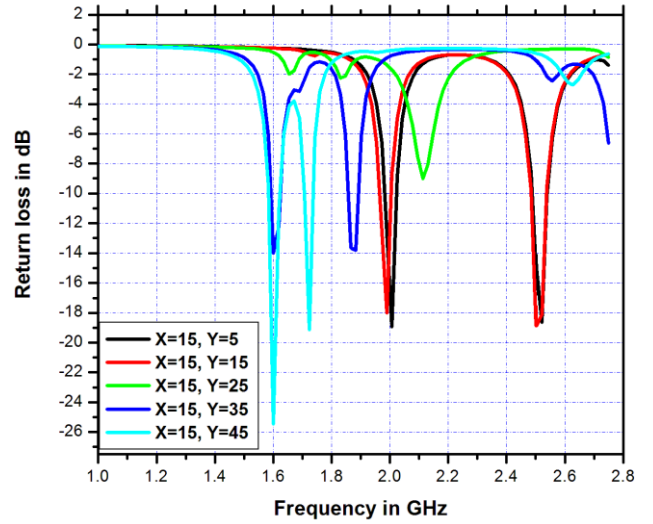


Fig. 3(b) Return loss plots of the patch antenna for X=15mm, Y=5, 15, 25, 35 and 45mm.

4.2 The Radiation Pattern

To observe the radiation pattern, we perform the experiment for different antennas with the required specific dimensions in the HFSS platform. For the patch having an incline slit at $p = 37\text{mm}$ and $\theta = 70^\circ$, the E-plane radiation patterns are shown in Fig. 4(a) through Fig.4 (e), and the H-plane radiation patterns are shown in Fig. 5 (a) through Fig.5 (e) for the extended patch dimensions of $(X=0, Y=0)$, $(X = 3, Y = 5)$, $(X = 3, Y = 45)$, $(X = 15, Y = 5)$ and $(X = 15, Y = 45)$ respectively. (\cdots 1st resonant frequency, — 2nd resonant frequency).

The current distributions over the patch at their resonant frequencies are shown in Fig.6 (a) through Fig.6 (f) for the patch having slit at $p = 37\text{mm}$ and $\theta = 70^\circ$ for extended dimensions $(X = 0, Y = 0)$, $(X = 3, Y = 5)$ and $(X = 15, Y = 5)$.

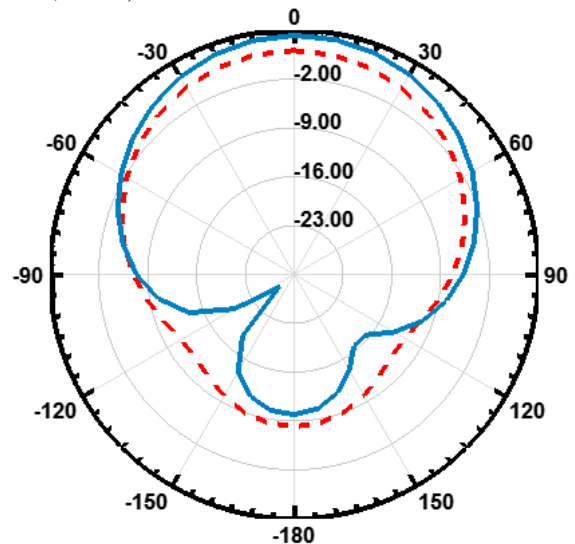


Fig. 4(a) E-plane for $f_1=1.95\text{GHz}$ $f_2=2.44\text{GHz}$ at dimension X=0mm, Y=0mm.

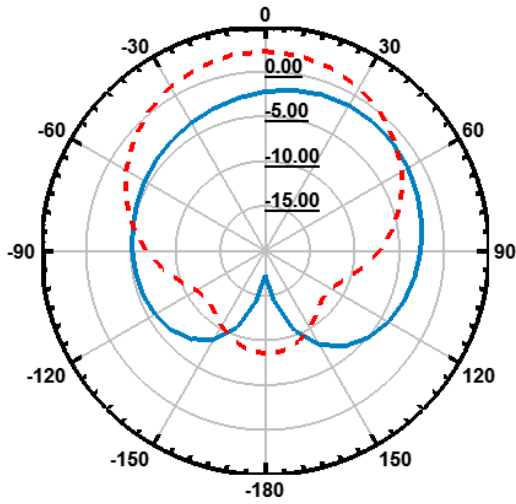


Fig. 4(b) E-plane for $f_1=2\text{GHz}$, $f_2=2.56\text{GHz}$ at dimension $X=3\text{mm}$, $Y=5\text{mm}$.

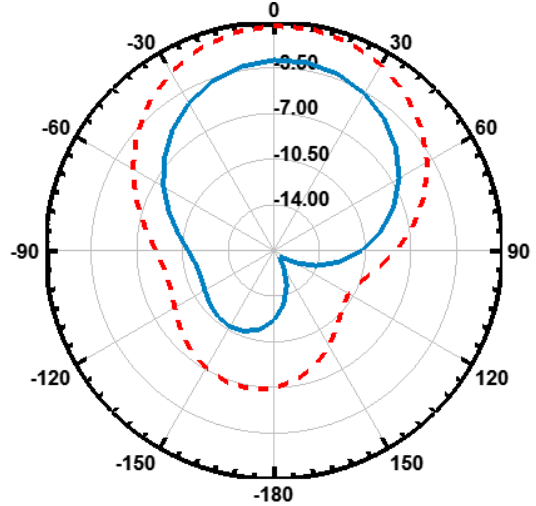


Fig. 4(e) E-plane for $f_1=1.6\text{GHz}$, $f_2=1.72\text{GHz}$ at dimension $X=15\text{mm}$, $Y=45\text{mm}$.

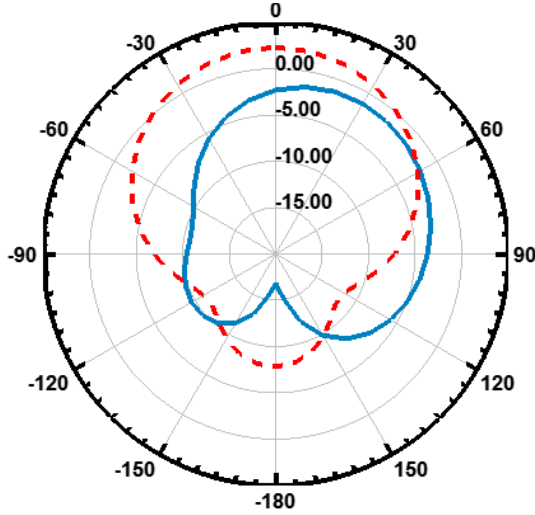


Fig. 4(c) E-plane for $f_1=1.97\text{GHz}$, $f_2=2.34\text{GHz}$ at dimension $X=3\text{mm}$, $Y=45\text{mm}$.

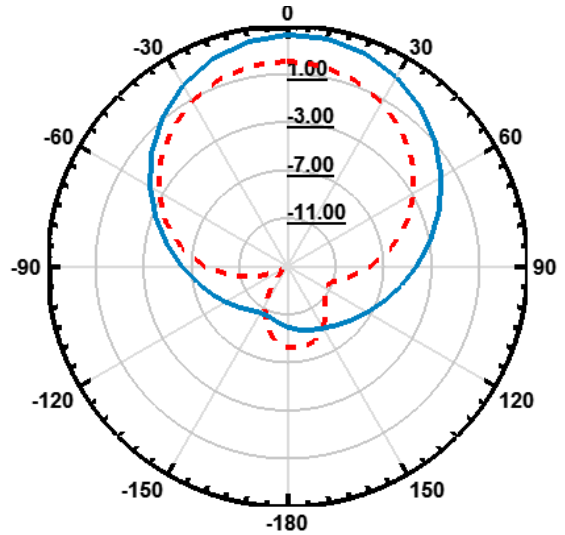


Fig. 5(a) H-plane for $f_1=1.95\text{GHz}$, $f_2=2.44\text{GHz}$ at dimension $X=0\text{mm}$, $Y=0\text{mm}$.

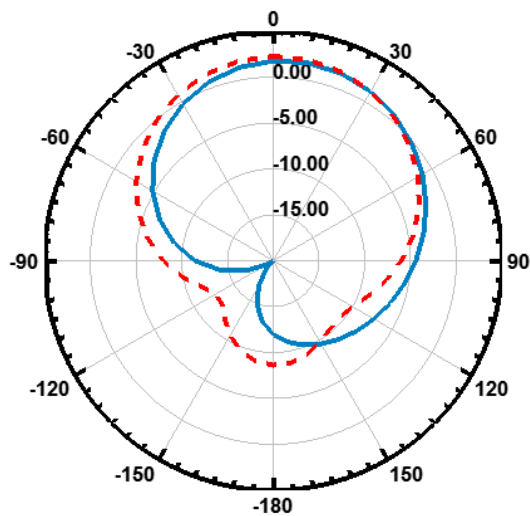


Fig. 4(d) E-plane for $f_1=2\text{GHz}$, $f_2=2.25\text{GHz}$ at dimension $X=15\text{mm}$, $Y=5\text{mm}$.

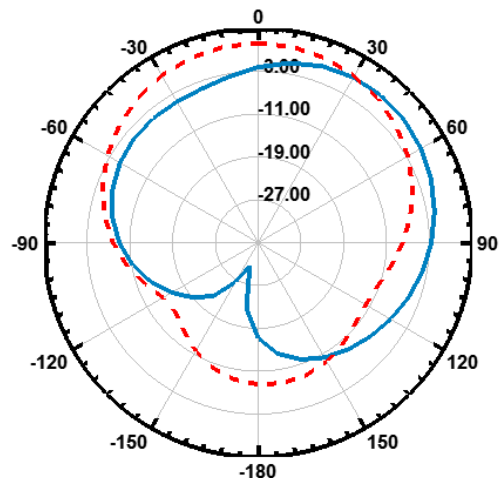


Fig. 5(b) H-plane for $f_1=2\text{GHz}$, $f_2=2.56\text{GHz}$ at dimension $X=3\text{mm}$, $Y=5\text{mm}$.

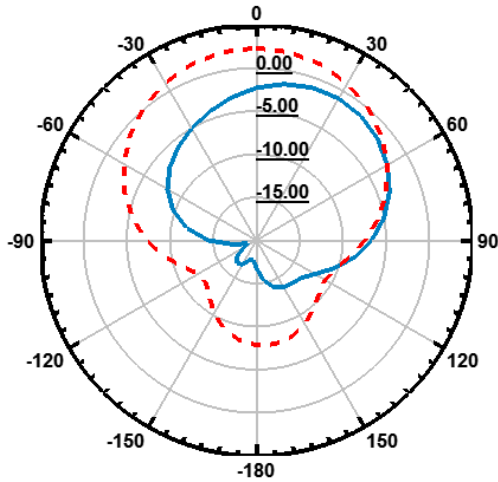


Fig. 5(c) H-plane for $f_1=1.97\text{GHz}$ $f_2=2.34\text{GHz}$ at dimension $X=3\text{mm}$, $Y=45\text{mm}$.

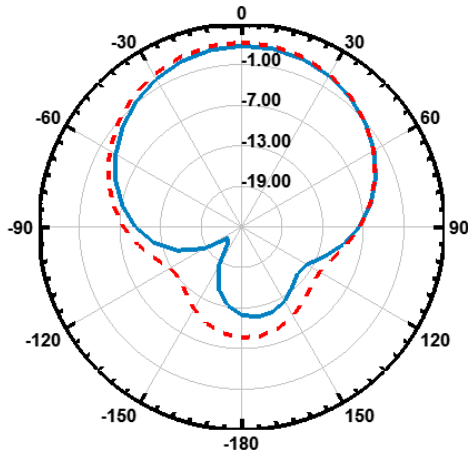


Fig. 5(d) H-plane for $f_1=2\text{GHz}$ $f_2=2.25\text{GHz}$ at dimension $X=15\text{mm}$, $Y=5\text{mm}$.

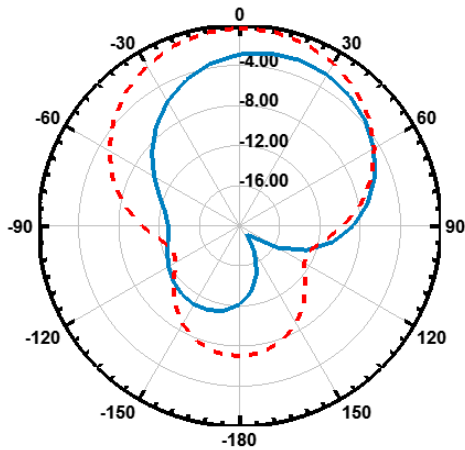


Fig. 5(e) H-plane for $f_1=1.6\text{GHz}$ $f_2=1.72\text{GHz}$ at dimension $X=15\text{mm}$, $Y=45\text{mm}$.

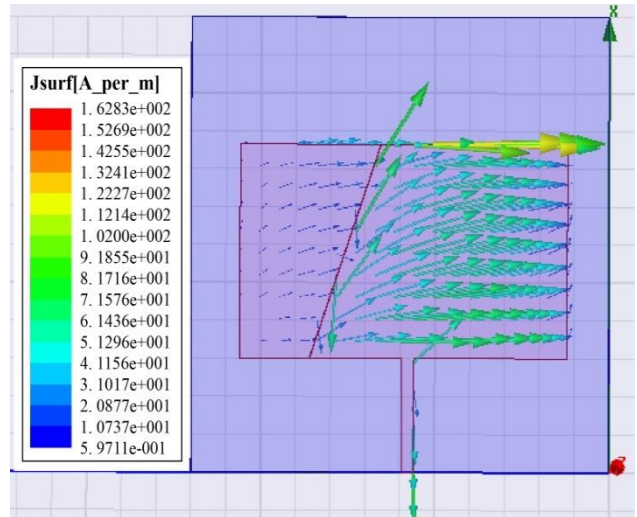


Fig. 6(a) Surface current distribution over the patch at 1.95GHz having $X=0\text{mm}$, $Y=0\text{mm}$.

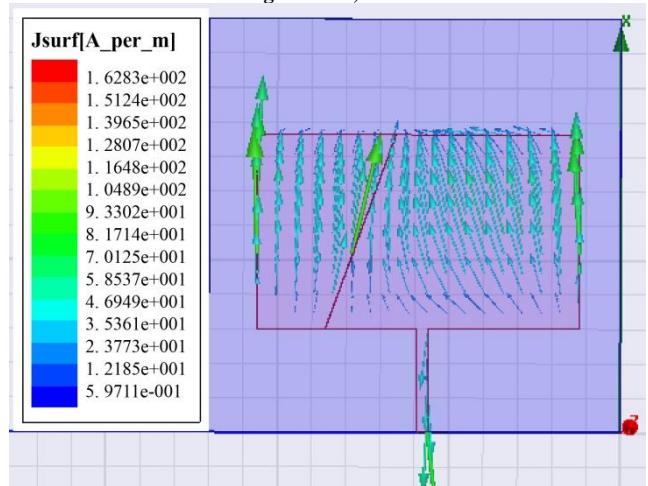


Fig. 6(b) Surface current distribution over the patch at 2.44GHz having $X=0\text{mm}$, $Y=0\text{mm}$.

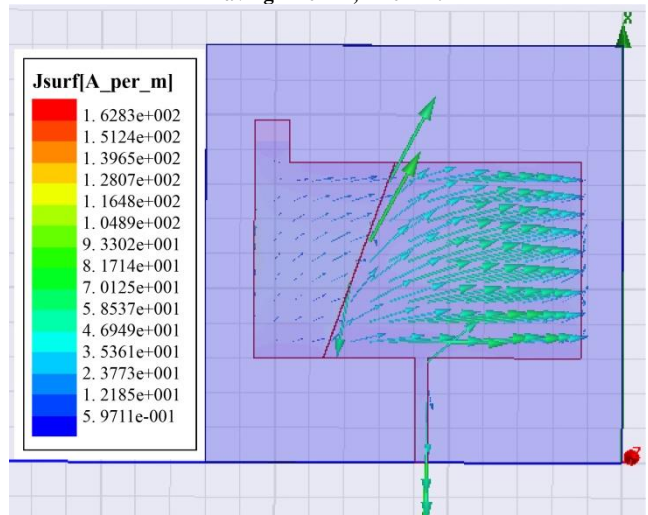


Fig. 6(c) Surface current distribution over the patch at 2.00GHz having $X=3\text{mm}$, $Y=5\text{mm}$.

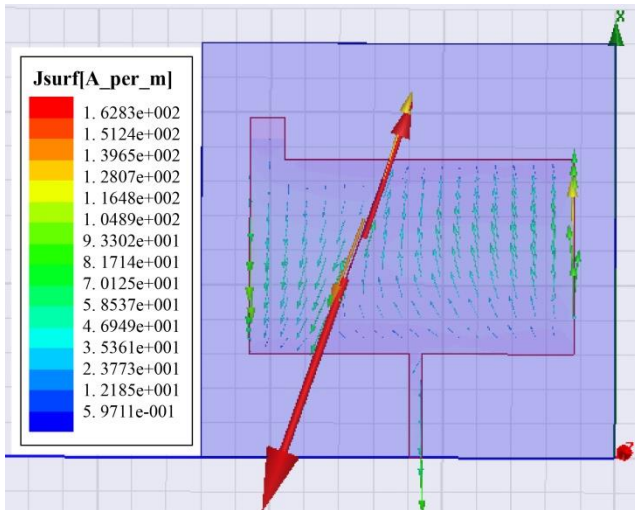


Fig. 6(d) Surface current distribution over the patch at 2.56GHz having X=3mm, Y=5mm.

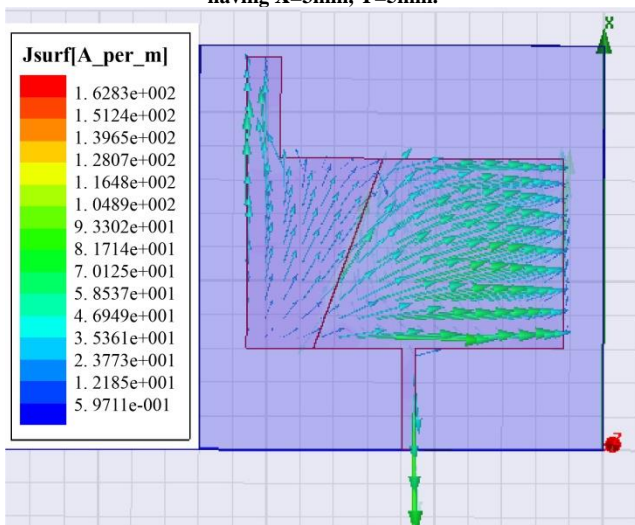


Fig. 6(e) Surface current distribution over the patch at 2.0GHz having X=15mm, Y=5mm.

For higher resonant frequency near 2.44GHz, the surface current direction is along the length of the patch. But, it is oriented along the width of the patch due to the insertion of the slit, which causes an increase in the average length of the current path. Due to the extension of the patch dimension and the insertion of the slit, the antenna's electrical length is increased, resulting in low-

References

- [1] Tilak Sarmah, Pranjal Borah, and Tulshi Bezboruah, "Design of a Dual-Band Rectangular Microstrip Patch Antenna With Diagonal Slit for Its Use in L- and S-Band Communications," *Advances in Communication, Devices and Networking*, vol. 537, 2019. *Crossref*, https://doi.org/10.1007/978-981-13-3450-4_18
- [2] Pranjal Borah, and Satyajib Bhattacharyya, "Design of a Dual Band V-Shaped Patch Antenna Using Shorting Posts," *Microwave and Optical Technology Letters*, vol. 58, no. 2, pp. 376-378, 2016. *Crossref*, <https://doi.org/10.1002/mop.29563>
- [3] T. Fujimoto, and K. Tanaka, "Stacked Square Microstrip Antenna with a Shorting Post for Dual Band Operation," *IEEE Antennas and Propagation Society International Symposium*, pp. 3585-3588, 2006. *Crossref*, <https://doi.org/10.1109/APS.2006.1711395>
- [4] Anjali Ashish Chaudhari, and Rajiv Kumar Gupta, "A Simple Tri-Band MIMO Antenna Using a Single Ground Stub," *Progress in Electromagnetics Research*, vol. 86, pp.191-201, 2018.
- [5] Xinbo Liu et al., "A Simple Dual-Band Antenna Using a Meander Line and a Tapered Rectangle Patch for WLAN Applications," *International Conference on Communication Problem-Solving, IEEE*, pp. 542-545, 2014. *Crossref*, <https://doi.org/10.1109/ICCPS.2014.7062341>

frequency radiation. The radiation pattern shows a broadside radiation pattern for both the E and H-plane in higher resonant frequency. At the same time, a back lobe pattern is observed at the lower resonant frequency.

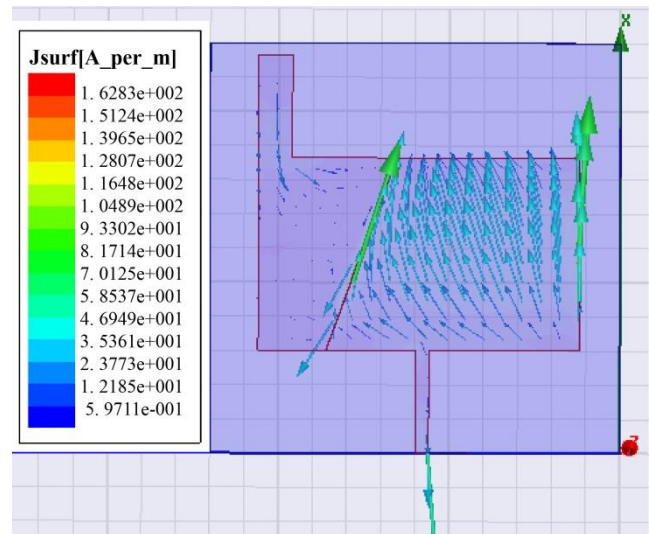


Fig. 6 (f) Surface current distribution over the patch at 2.25GHz having X=15mm, Y=5mm.

5. Conclusion

The observed results show that by the introduction of the slit, dual frequency operation can be achieved. By adding an extra portion to the patch's upper end, we can achieve dual frequency tuning. In our proposed design, it is possible to tune in the upper frequency from 1.72GHz ($S_{11} = -19.14\text{dB}$, Gain = 1.8dB) to 2.56GHz ($S_{11} = -17.73\text{dB}$, Gain = 4.67dB) and lower frequency from 1.6GHz ($S_{11} = -25.47\text{dB}$, Gain = 1.85dB) to 2.00GHz ($S_{11} = -16.80\text{dB}$, Gain = 4.31dB). Tuning of MSA with PIN diode, varactor diode etc., are very complex processes where an external circuit is required. Our proposed tuning technique is the simplest one. In our future work, we propose to fabricate a dual-band microstrip antenna, and for tuning operation, we will use linear gear and pulley system to tune it mechanically.

Acknowledgement

The authors are thankful to the Head of the Dept. of Electronics and Communication Technology, Gauhati University, Assam, India, for providing valuable suggestions and laboratory infrastructure during the work.

- [6] F. N. M. Redzwan et al., "Dual-Band Planar Inverted F Antenna With Parasitic Element for LTE and WIMAX Mobile Communication," *International Symposium on Technology Management and Emerging Technologies*, pp. 62-67, 2014. *Crossref*, <https://doi.org/10.1109/ISTMET.2014.6936478>
- [7] Mr. Navneet Kumar, and Dr. Narinder Sharma, "The Various Feeding Techniques of Microstrip Patch Antenna Using HFSS," *SSRG International Journal of Electronics and Communication Engineering*, vol. 6, no. 6, pp. 23-29, 2019. *Crossref*, <https://doi.org/10.14445/23488549/IJECE-V6I6P106>
- [8] Ketavath Kumar Naik et al., "Enhancement of Gain with Corrugated Y-Shaped Patch Antenna for Triple-Band Application," *International Journal of RF and Microwave Computer-Aided Engineering*, vol. 29, no. 3, pp. 21-24, 2019. *Crossref*, <https://doi.org/10.1002/mmce.21624>
- [9] J. A. Anasri, Satya Kesh Dubey, and Prabhakar Singh, "Analysis of U-Slot Loaded Patch for Dual Band Operation," *International Journal of Microwave Optical Technology Letters*, vol. 3, pp. 80-84, 2008.
- [10] Javad Ghalibafan, Amir Attari, and Farrokh Hojjat-Kashani, "A New Dual-Band Microstrip Antenna With U-Shaped Slot," *Progress in Electromagnetics Research*, vol. 12, pp. 215-223, 2010. *Crossref*, <http://dx.doi.org/10.2528/PIERC10012706>
- [11] Yun Liu, Zhenyi Niu, and Xiaojun Wang, "Design of Dual-Band H-Shaped Slot Antenna for 2.4 and 5 Ghz Wireless Communication," *International Conference on Microwave Technology and Computational Electromagnetics (ICMTCE 2009)*, pp. 95-97, 2009. *Crossref*, <https://doi.org/10.1049/cp.2009.1264>
- [12] Ranjeet Singh, and Dr. Simranjeet Singh Tiwana, "Design and Performance of a Compact Microstrip Patch Antenna Using Circular Slots and Stub for RFID Applications," *SSRG International Journal of Electronics and Communication Engineering*, vol. 4, no. 8, pp. 1-6, 2017. *Crossref*, <https://doi.org/10.14445/23488549/IJECE-V4I8P101>
- [13] Bondili Siva Hari Prasad, and Mokkaat Venkata Prasad, "Design and Analysis of Compact Periodic Slot Multiband Antenna with Defected Ground Structure for Wireless Applications," *Progress in Electromagnetic Research*, vol. 93, pp. 77-87, 2020. *Crossref*, <http://dx.doi.org/10.2528/PIERM20032605>
- [14] Ravikumar, and Dattatreya Gopi, "Design of Quad Band Microstrip Patch Antenna with Slits and Slots," *International Journal of Advance Technology and Engineering Exploration*, vol. 8, no. 82, pp.1234-1242, 2021.
- [15] Hussain Hammas, Mohammed Hasan, and Ali Jalal, "Compact Multiband Microstrip Printed Slot Antenna Design for Wireless Communication Applications," *Advanced Electromagnetics*, vol. 9, no. 2, pp. 52-59, 2020. *Crossref*, <https://doi.org/10.7716/aem.v9i2.1393>
- [16] Xi-Wang Dai et al., "Multiband and Dual-Polarized Omnidirectional Antenna for 2G/3G/LTE Application," *IEEE Antennas and Wireless Propagation Letters*, vol. 12, pp. 1492-1495, 2013. *Crossref*, <https://doi.org/10.1109/LAWP.2013.2289743>
- [17] R.Anbu, and A.Jayakumar, "Design and Analysis of Array Microstrip Patch Antenna with Frequency Reconfiguration," *SSRG International Journal of Electronics and Communication Engineering*, vol. 4, no. 4, pp. 1-4, 2017. *Crossref*, <https://doi.org/10.14445/23488549/IJECE-V4I4P101>
- [18] Premavani, C. Kalpana, and S.N. Mulgi, "Design and Development of Inverted U-Slot Rectangular Ring Coupled Monopole Microstrip Antenna for Quad Band Operation," *International Journal for Research in Applied Science and Engineering Technology (IJRASET)*, vol. 9, no. 12, pp. 1394-1397, 2021.
- [19] Shobhit Kumar Patel, Christos Argyropoulos, and Yogeshwar P. Kosta, "Pattern Controlled and Frequency Tunable Microstrip Antenna Loaded With Multiple Split Ring Resonators," *IET Microwaves, Antennas & Propagation*, vol. 12, no. 3, pp. 390-394, 2018. *Crossref*, <https://doi.org/10.1049/iet-map.2017.0319>
- [20] Amit A. Deshmukh et al., "Analysis of Stub Loaded Rectangular Microstrip Antenna," *2012 National Conference on Communications (NCC)*, 2012. *Crossref*, <https://doi.org/10.1109/NCC.2012.6176802>
- [21] B. Vedaprabhu, and K.J. Vinoy, "A Double U-Slot Patch Antenna with Dual Wideband Characteristics," *2010 National Conference On Communications (NCC) IEEE*, 2010. *Crossref*, <https://doi.org/10.1109/NCC.2010.5430170>
- [22] R. N. Simons, Donghoon Chun, and L.P.B. Katehi, "Microelectromechanical Systems (MEMS) Actuators for Antenna Reconfigurability," *2001 IEEE MTT-S International Microwave Symposium Digest (Cat. No.01CH37157)*, pp. 215-218. *Crossref*, <https://doi.org/10.1109/MWSYM.2001.966874>
- [23] Veeresh G. Kasabegoudar, "Analysis of Coplanar Capacitive Coupled Wideband Microstrip Antennas," *International Journal of Engineering Trends and Technology*, vol. 69, no. 9, pp. 45-50, 2021. *Crossref*, <https://doi.org/10.14445/22315381/IJETT-V69I9P206>
- [24] Symeon Nikolaou et al., "Pattern and Frequency Reconfigurable Annular Slot Antenna Using PIN Diodes," *IEEE Transactions on Antennas and Propagation*, vol. 54, no. 2, pp. 439-448, 2006. *Crossref*, <https://doi.org/10.1109/TAP.2005.863398>
- [25] N. Behdad, and K. Sarabandi, "A Varactor-Tuned Dual-Band Slot Antenna," *IEEE Transactions on Antennas and Propagation*, vol. 54, no. 2, pp. 401-408, 2006. *Crossref*, <https://doi.org/10.1109/TAP.2005.863373>
- [26] Prasad N. Shastry, and Krishna Katragadda, "Design Guidelines for a Novel Tunable Aperture Coupled Microstrip Patch Antenna," *IEEE International Symposium on Antenna and Propagation*, pp. 913-914, 2019. *Crossref*, <https://doi.org/10.1109/APUSNCURSINRSM.2019.8889311>
- [27] Girish Bhide et al., "FDTD Analysis of Union-Shaped Triple Band Microstrip Patch Antenna Using the Novel Algorithm for Identification of Contiguous White Pixels in a Column of an Image," *International Journal of Engineering Trends and Technology*, vol. 70, no. 12, pp. 90-98, 2022. *Crossref*, <https://doi.org/10.14445/22315381/IJETT-V70I12P210>

- [28] Parimita Saikia, and Anup Kr Bordoloi, "Study of Modified Rectangular Patch Antenna for Tuning Resonant Frequency in S-Band," *International Conference on Advanced Computational and Communication Paradigms (ICACCP)*, 2019. *Crossref*, <https://doi.org/10.1109/ICACCP.2019.8883001>
- [29] Md. Naimur Rahman et al., "A Tuning Fork-Shaped Microstrip Patch Antenna for X-Band Satellite and Radar Applications," *International Conference on Electrical Engineering and Informatics, ICEEI*, 2017. *Crossref*, <https://doi.org/10.1109/ICEEI.2017.8312440>
- [30] Prasad N. Shastry, and Aparna Sankarasubramaniam, "Design Optimization of a Tunable Coplanar Patch Antenna," *IEEE International Symposium on Antennas and Propagation and North America Radio Science Meeting*, 2020. *Crossref*, <https://doi.org/10.1109/IEEECONF35879.2020.9329868>
- [31] Elliot O. Omoru, and Viranjay M. Srivastava, "Bandwidth and Return Loss Improvement Technique Using Doublematerial Substrate Cylindrical Surrounding Patch Antenna:Parti," *International Journal of Engineering Trends and Technology*, vol. 69, no. 12, pp. 252-256, 2021. *Crossref*, <https://doi.org/10.14445/22315381/IJETT-V69I12P230>
- [32] K. Joe et al., "Frequency Tunable Monopole Patch Antenna Using Broadside Coupled Split Ring Resonator for Wireless Communication Applications," *International Congress on Artificial Materials for Novel Wave Phenomena-Metamaterials*, 2019. *Crossref*, <https://doi.org/10.1109/MetaMaterials.2019.8900946>
- [33] Shi-Chang Tang, Xue-Ying Wang, and Jian-Xin Chen, "Low-Profile Frequency- Reconfigurable Dielectric Patch Antenna and Array Based on New Varactor Loading Scheme," *IEEE Transaction on Antenna and Propagation*, vol. 69, no. 9, 2021. *Crossref*, <https://doi.org/10.1109/TAP.2021.3060053>
- [34] Payam Nayeri, and Randy Haupt, "A Mechanically Configurable Microstrip Patch Antenna for IEEE 802.11 WLAN Band," *United States National Committee of URSI National Radio Science Meeting*, 2019. *Crossref*, <https://doi.org/10.23919/USNC-URSI-NRSM.2019.8713027>
- [35] Pranav Bhatt et al., "Microstrip-Fed 3.04 -10.77 Ghz UWB Patch Antenna Design Using CMA and Parametric Study," *International Journal of Engineering Trends and Technology*, vol. 70, no. 7, pp. 250-259, 2022. *Crossref*, <https://doi.org/10.14445/22315381/IJETT-V70I7P225>
- [36] Javad Ghalibafan, Amir Attari, and Farrokh Hojjat-Kashani, "A New Dual-Band Microstrip Antenna with U-Shaped Slot," *Progress in Electromagnetic Research*, vol. 12, pp. 215-223, 2010. *Crossref*, <http://dx.doi.org/10.2528/PIERC10012706>
- [37] A. V. Gevorkyan, "The Dual-Band Patch Antenna," *In Radiation and Scattering of Electromagnetic Waves, RSEMW*, pp. 306-308, 2017. *Crossref*, <https://doi.org/10.1109/RSEMW.2017.8103657>
- [38] Ravikumar Palla, and Kumar Naik Ketavath, "Multiband Rectangular Microstrip Patch Antenna Operating At C, X and Ku Bands," *International Conference on Multimedia Processing, Communication and Information Technology, IEEE*, pp. 19-25, 2020. *Crossref*, <https://doi.org/10.1109/MPCIT51588.2020.9350318>
- [39] Moh. Amanta K. S. Lubis, Fitri Yuli Zulkifli, and Eko Tjipto Rahardjo, "Design of Multi Band Microstrip Antenna for Industrial, Scientific and Medical Band Application," *International Symposium on Electronics and Smart Devices (ISESD)*, pp. 343-346, 2016. *Crossref*, <https://doi.org/10.1109/ISESD.2016.7886745>
- [40] Emre Erdil et al., "Frequency Tunable Microstrip Patch Antenna Using RF MEMS Technology," *IEEE Transactions on Antennas and Propagation*, vol. 55, no. 4, pp. 1193–1196, 2007. *Crossref*, <https://doi.org/10.1109/TAP.2007.893426>
- [41] F.A. Asadallah et al., "A Digitally Tuned Reconfigurable Patch Antenna for IoT Devices," *IEEE International Symposium on Antenna and Propagation*, pp. 917-918, 2017. *Crossref*, <https://doi.org/10.1109/APUSNCURSINRSM.2017.8072501>
- [42] Nguyen Minh Tan et al., "Shroted Patch Antenna With Tuning Slit for RFID Tag Mounted on Metallic Plane," *International Workshop on Electromagnetics: Applications and Student Innovation Competition (IWEM)*, 2020. *Crossref*, <https://doi.org/10.1109/iWEM49354.2020.9237412>
- [43] Constantine A. Balanis, *Antenna Theory Analysis and Design*, 3rd Edition Wiley-Interscience, pp. 810-817, 2005.